

Efficient Human Pose Estimation with Depthwise Separable Convolution and Person Centroid Guided Joint Grouping

Jie Ou and Hong Wu

School of Computer Science and Engineering,
University of Electronic Science and Technology of China,
Chengdu 611731, China
oujieww6@gmail.com, hwu@uestc.edu.cn

Abstract. In this paper, we propose efficient and effective methods for 2D human pose estimation. A new ResBlock is proposed based on depthwise separable convolution and is utilized instead of the original one in Hourglass network. It can be further enhanced by replacing the vanilla depthwise convolution with a mixed depthwise convolution. Based on it, we propose a bottom-up multi-person pose estimation method. A rooted tree is used to represent human pose by introducing person centroid as the root which connects to all body joints directly or hierarchically. Two branches of sub-networks are used to predict the centroids, body joints and their offsets to their parent nodes. Joints are grouped by tracing along their offsets to the closest centroids. Experimental results on the MPII human dataset and the LSP dataset show that both our single-person and multi-person pose estimation methods can achieve competitive accuracies with low computational costs.

Keywords: Human Pose Estimation · Depthwise separable convolution · Hourglass network · Joint Grouping

1 Introduction

Human pose estimation aims to locate human body joints from a single monocular image. It is a challenge and fundamental task in many visual applications, e.g. surveillance, autonomous driving, human-computer interaction, etc. In the last few years, considerable progress on human pose estimation has been achieved by deep learning based approaches [17,34,29,18,19,35].

Most existing research works on human pose estimation focus on improving the accuracy and develop deep networks with large model size and low computational efficiency, which prohibits their practical application. To adopt deep networks in real-time applications and/or on limited resource devices, the model should be compact and computational efficient. Inception module [30] is used to build deeper networks without increase model size and computational cost. Depthwise separable convolution [5,10,31], has been utilized as the key building

block in many successful efficient CNNs. In this paper, we follow these successful design principles to develop efficient deep networks for human pose estimation.

For multi-person pose estimation, it is needed to distinguishing poses of different persons. The approaches can mainly be divided into two categories: top-down strategy and bottom-up strategy. The top-down approaches [22,13,6,34,29] employ detectors to localize person instances and then apply joint detector to each person instance. Each step of top-down approaches requires a very large amount of calculations, and the run-time of the second step is proportional to the number of person. In contrast, the bottom-up approaches [21,24,15,12,11,3] detect all the body joints for only once and then group/allocate them into different persons. However, they suffer from very high complexity of joint grouping step, which usually involves solving a NP-hard graph partition problem. Different methods have been proposed to reduce the grouping time. Recently, some one-stage multi-person pose estimation approaches [19,27,32] have been proposed, but their performance lag behind the two-stage ones. In this paper, we also focus on the bottom-up strategy.

In this paper, we propose efficient and effective methods for 2D human pose estimation. A new ResBlock is proposed with two depthwise separable convolutions and a squeeze-and-excitation (SE) module and utilized in place of the original ResBlock in Hourglass network. Its representation capability is further enhanced by replacing the vanilla depthwise convolution with a mixed depthwise convolution. The new Hourglass networks is very light-weighted and can be directly applied to single-person pose estimation. Base on this backbone network, we further propose a new bottom-up multi-person pose estimation method. A rooted tree is used to represent human pose by introducing person centroid as the root which connecting to all the joints directly or hierarchically. Two branches of sub-networks are used to predict the centroids, body joints and their offsets to their parent nodes. Joints are grouped by tracing along their offsets to the closest centroids. Our single-person pose estimation method is evaluated on MPII Human Pose dataset [1] and Leeds Sports Pose dataset [14]. It achieves competitive accuracy with only 4.7 GFLOPs. Our multi-person pose estimation method is evaluated on MPII Human Pose Multi-Person dataset [1], and achieves competitive accuracy with only 13.6 GFLOPs.

2 Related Works

2.1 Efficient Neural Networks

To adopt deep neural networks in real-time applications and/or on resource-constrained devices, many research works have been devoted to build efficient neural networks with acceptable performance. Depthwise separable convolution was originally presented in [28]. It can achieve a good balance between the representation capability and computational efficiency, and has been utilized as the key building block in many successful efficient CNNs, such as Xception [5], MobileNets [10,26] and ENAS [23]. MixConv [31] extends vanilla depthwise con-

volution by partitioning channels into multiple groups and apply different kernel sizes to each of them, and achieves better representation capability.

2.2 Multi-person pose estimation

Top-down methods. Top-down multi-person pose estimation methods first detect people by a human detector (*e.g.* Faster-RCNN[25]), then run a single-person pose estimator on the cropped image of each person to get the final pose predictions. Representative top-down methods include PoseNet [22], RMPE [6], Mask R-CNN [8], CPN [4] and MSRA [34]. However, top-down methods depend heavily on the human detector, and their inference time will significantly increase if many people appear together.

Bottom-up methods. Bottom-up methods detect the human joints of all persons at once, and then allocate these joints to each person based on various joint grouping methods. However, they suffer from very high complexity of joint grouping step, which usually involves solving a NP-hard graph partition problem. DeepCut [24] and DeeperCut [12] solve the joint grouping with an integer linear program which results in the order of hours to process a single image. Later works drastically reduce prediction time by using greedy decoders in combination with additional tools. Cao *et al.* [3] proposed part affinity fields to encode location and orientation of limbs. Newell and Deng [16] presented the associative embedding for grouping joint candidates. PPN [18] performs dense regressions from global joint candidates within a embedding space of person centroids to generate person detection and joint grouping. But it need to adopt the Agglomerative Clustering algorithm [2] to determine the person centroids. In this paper, we avoid the time-consuming clustering by regressing the person centroids together with body joints and using them to guide the joint grouping.

Recently, Nie *et al.* [19] proposed a one-stage multi-person pose estimation method (SPM) which predicts root joints (person centroids) and joint displacements directly. Although both SPM and our method predict person centroid, they use centroid plus displacements to recover joints and we use centroid to guide joint grouping. We argue that joints can be predicted more precisely than its displacements.

3 The proposed light-weight Hourglass network

3.1 Hourglass network

Although Hourglass network has been utilized in many human pose estimation methods [35,20,18,19], it is hard to been adapted in practical applications due to its large model size. Original Hourglass network consists of eight stacked hourglass modules, whose structure is illustrated in Fig. 1. The ResBlock used in original Hourglass network has a bottleneck structure (Fig. 2(a)). In this paper, we try to improve the efficiency of Hourglass network by replacing the original ResBlocks with the light-weight ones (Fig. 1). The proposed Hourglass network is called DS-Hourglass network. More details are given as follows.

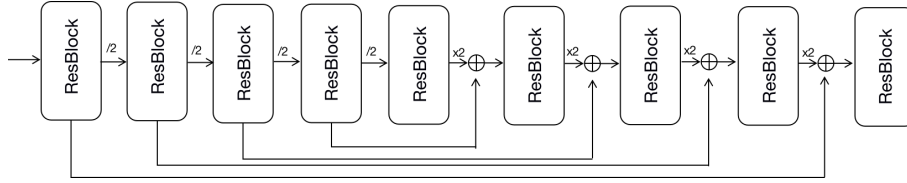


Fig. 1. An illustration of a Hourglass module, “/2” means downsampling operation and “x2” means upsampling operation.

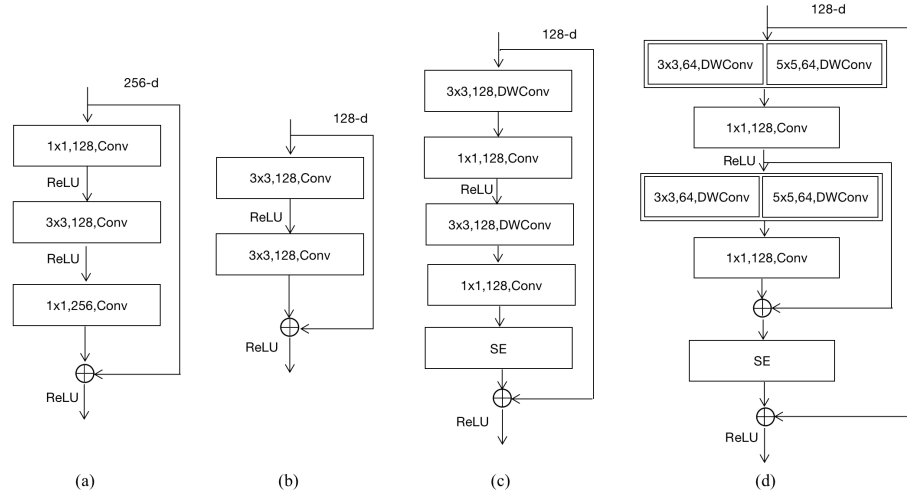


Fig. 2. Architecture of the ResBlocks. (a) The original ResBlock in Hourglass[17]. (b) another kind of ResBlock proposed in ResNet[9]. (c) DS-ResBlock corresponding to (b), (d) replace the DWConv in (c) with Mix-Cov.

3.2 Depthwise Separable Convolutions

A depthwise separable convolution decomposes a standard convolutional operation into a depthwise convolution (capture the spatial correlation) followed by a pointwise convolution (capture the cross-channel correlation).

A standard convolution operation needs $c_1 \times c_2 \times k \times k$ parameters and about $h \times w \times c_1 \times c_2 \times k \times k$ computational cost, where $h \times w$, c_1/c_2 and $k \times k$ are the spatial size of input and output feature maps, the number of input/output feature channels and the convolutional kernel size, respectively. While a depthwise separable convolution operation only needs $c_1 \times k \times k + c_1 \times c_2$ parameters and about $h \times w \times c_1(k^2 + c_2)$ computational cost. For example, if we set k to 3 and c_2 to 128, the number of parameters and the computational cost of the depthwise separable convolution is only about 1/9 of the corresponding standard convolution.

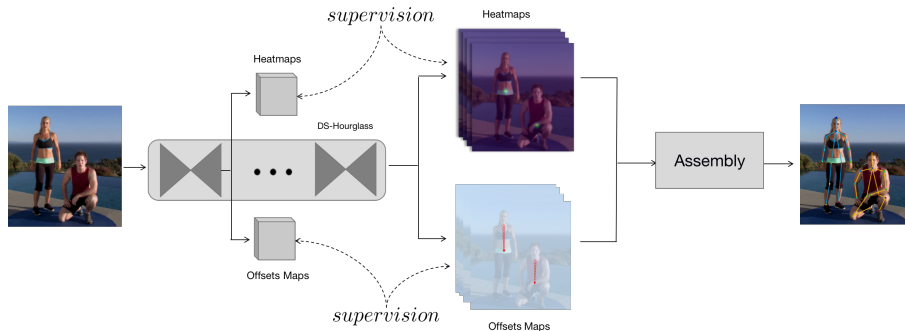


Fig. 3. Our pipeline. Our method takes color image as input, the DS-Hourglass build with 8 stage and predict 2 sets, heatmaps and offsetmaps, finally return joints for each person in image at once by our efficient joint grouping algorithm.

3.3 Light-weight ResBlock

To develop efficient ResBlock, we first reduce the number of its input/output feature channels from 256 to 128, and use two stacked 3×3 convolutions (Fig. 2(b)). Then, we replace the two standard 3×3 convolutions with two depthwise separable convolutions followed with a squeeze-and-excitation (SE) block to get a light-weight ResBlock (Fig. 2(c)). The SE block is very efficient and used to relocate features and strengthen features. To capture the information of different scales, we further replace the depthwise convolution with a mixed depthwise convolution (MixConv [31]) to get another version of light-weight ResBlock (Fig. 2(d)). In MixConv, the input feature channels are first split into groups, then depthwise convolutions with different kernel sizes are applied to different groups, finally, the output of each depthwise convolution are concatenated. In this paper, we apply kernels of 3×3 and 5×5 to two groups of channels respectively to trade-off the representation capability and the computational costs. In our study, we found that adding a skip connection around the second depthwise separable convolution can make the training of this ResBlock (Fig. 2(d)) more stable.

4 Multi-Person Pose Estimation

Fig. 3 illustrates the overall pipeline of our network. Our multi-person pose estimation method first predicts joints of all person at once, then the joint candidates are grouped into different persons. To improve the efficiency of joint grouping, a rooted tree is used to represent human pose by using person centroid as the root which connecting to all the joints directly or hierarchically. Another network branch is used to predict the offset from each joint to its parent node. The person centroid is treated as a pseudo joint and predicted together with body joints. After that, body joints are grouped by tracing along their offsets to the closed centroids.

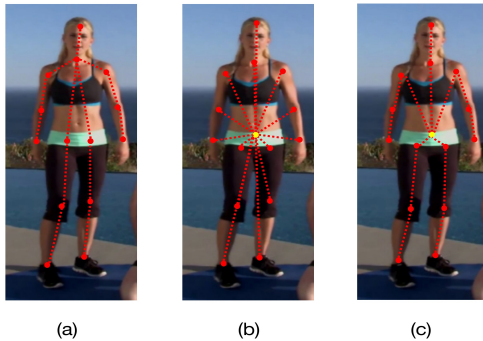


Fig. 4. Pose representations: (a) kinematic structure; (b) centroid-rooted tree; (c) heirarchical centroid-rooted tree

4.1 Centroid-rooted tree structure to define the offsets

The centroid-rooted tree structure is illustrated in Fig. 4(b), where the person centroid (root node) directly connect to all body joints (leaf nodes). The drawback of this representation is that it leads to some long-range offsets which are hard to be precisely predicted, e.g. from ankle, knee and wrist to the centroid. To alleviate this problem, we further proposed a hierarchical centroid-rooted tree (Fig. 4(c)) based on the kinematic structure (Fig. 4(a)), where the long-range offsets are decomposed into short-range or middle-range offsets.

4.2 Joint and Offset Prediction

Our network has two branches of sub-networks for joint and offset prediction. Both sub-networks have only one 1×1 convolution and share the same feature maps from hourglass module.

Joint Prediction. Our ground-truth heatmap is generated according to following equation,

$$H_j(x, y) = \min\left(\sum_{i=1}^N \exp\left(-\frac{((x, y) - (x_j^i, y_j^i))^2}{2\sigma^2}\right), 1\right), \quad (1)$$

where (x_j^i, y_j^i) is the coordinate of joint j of person i , N is the number of person in the image and σ controls the spread of the peak, and minimum function is used to guarantee the value not greater than 1.

Offset Prediction. we construct a dense offset map for each body joint as the ground-truth for offset prediction. We first construct a offset map O_j^i for joint j of person i as:

$$O_j^i(x, y) = \begin{cases} \frac{1}{Z}((x_c^i, y_c^i) - (x, y)) & \text{if } (x, y) \in N_j^i \\ 0 & \text{otherwise} \end{cases} \quad (2)$$

where $N_j^i = \{(x, y) | \sqrt{(x, y) - (x_j^i, y_j^i)} \leq \tau\}$ denotes the area of neighbors of joint j of person i , (x_c^i, y_c^i) is the coordinate of the centroid of the person i , $Z = \frac{1}{2} \min(W, H)$ is a normalization coefficient, W and H are the width and height of the input image. If a location belongs to multiple people, these vectors are averaged. If the hierarchical centroid-rooted tree is used to represent human pose, we only need to replace the centroid in equation (2) with the parent node of the joint j of the person i .

The MSE Loss is used for joint prediction, and Smooth L1-Loss is used for offset prediction.

4.3 Centroid-guided joint grouping

Based on the predicted person centroids, we develop a greedy method for joint grouping. First, we apply NMS to the heatmaps of the last stage of DS-Hourglass to get the coordinates of all candidate joints, and sort them in descending order of their score. For the centroid-rooted tree representation, joint allocation is performed independently for each body joint. Given a candidate of joint j , its centroid’s coordinate can be predicated as

$$(\hat{x}, \hat{y})_c = (x, y) + Z \times O_j(x, y), \quad (3)$$

where (x, y) is the coordinate of the candidate joint, $(\hat{x}, \hat{y})_c$ is the predicated coordinate of its person centroid, and O_j is the offset map of joint j . Then the predicated centroid is compared to each person centroid generated from heatmap and allocated to the nearest one under the constrain that one person has only one instance for each joint category.

For hierarchical centroid-rooted tree representation, the joints are also grouped hierarchically. Base on the intuition that the joints close to the torso can be predicted more reliably. We classify joints into three levels, the first level contains *shoulder*, *hip*, and *neck*, the second level contains *head*, *elbow* and *knee*, and third level contains *wrist* and *ankle*. The joint allocation is performed from the first level to the third level, each joint candidate is associated to its parent node in the tree structure according to equation (3) and the nearest-neighbour rule.

5 Experiments

5.1 Experiment setup

Datasets MPII Single-Person Dataset consists of around 25k images with annotations for multiple people providing 40k annotated samples (28k training, 11k testing) for single-person pose estimation. The MPII Multi-Person dataset consists of 3,844 and 1,758 groups of multiple interacting persons for training and testing. The LSP dataset has 11K training samples and 1K test samples, with 14 annotated joints for a person.

Table 1. Comparison of ResBlocks on MPII single-person validation set

Methods	Mean	Stages	Param	FLOPs
Hourglass [17]	90.52	8	26M	26.2G
SBN [34]	89.6	-	68.6M	21G
HRNet [29]	90.3	-	28.5M	9.5G
FPD [35]	89.04	4	3M	3.6G
DS-Hourglass*	88.71	8	2.9M	3.3G
DS-Hourglass w/o SE	89.47	8	2.9M	4.7G
DS-Hourglass	89.87	8	4.2M	4.7G
DS-Hourglass(mix)	89.94	8	4.6M	4.8G

Table 2. Comparison of assembly methods on MPII multi-person validation set

Model	Stage	Method	Mean	Param	FLOPs
Hourglass	8	PPN [18]	79.4	22M	62.9G
Hourglass	1	PPN	74.4	3.0M	10.8G
Hourglass	1	Center	75.8	3.0M	10.9G
Hourglass	1	Cent.Hier.	76.2	3.0M	10.9G
DS-Hourglass	8	Cent.Hier.	78.8	4.4M	13.3G
DS-Hourglass(mix)	8	Cent.Hier.	79.8	4.6M	13.6G

Training Details We randomly augmente the samples with rotation degrees in $[-40, 40]$, scaling factors in $[0.7, 1.3]$, translation offset in $[-40, 40]$ and horizontally mirror, adopt 256×256 as training size. The initial learning rate is 0.0025, learning rate decay at step 150, 170, 200 and 230 with total 250 epochs by 0.5.

5.2 Ablation Study

Ablation for ResBlocks In Table 1, DS-Hourglass* uses Fig. 2(c) with only one depthwise separable convolution. DS-Hourglass w/o SE uses Fig. 2(c) without SE module. DS-Hourglass and DS-Hourglass(mix) use Fig. 2(c) and Fig. 2(d) respectively. ResBlock with two depthwise separable convolution can improve 1.1% in PCKh than ResBlock with only one, but with 1.4 GFLOPs computational cost increased. SE model can imporve 0.4% in PCKh; Mixed depthwise convolution only bring very little improvement for single-person pose estimation. Compared with the excellent methods, our DS-Hourglass(mix) is 0.9% higher than FPD. And 0.36% lower than HRNet [29], However, the GFLOPs is only half of it and the parameters are only 16% of HRNet.

Ablation for Assembly methods Table 2 indicated that our centroid-guided method improves 0.4% over PPN, and our hierarchical centroid-guided method improves 1.8% over PPN. DS-Hourglass(mix) improves 1% over DS-Hourglass with hierarchical centroid-guided assembly method, as it can handles multi-scale problem better, even better than PPN [18] based on original Hourglass one (79.8% vs 79.4%), we can save 50GFLOPs and only need 21% parameters of PPN.

Table 3. Result on MPII Single-Person test set. * means the use of extend dataset.

Method	PCKh	Auxiliaries	Stage	Pre.	Input size	Out. size	FLOPs	#Param
DeeperCut [12]	88.5	-	-	yes	344×344	43×43	37G	66M
CPM* [33]	88.5	-	6	yes	368×368	46×46	175G	31M
SHG [17]	90.9	-	8	no	256×256	64×64	26.2G	26M
PIL [20]	92.4	Segment	8	no	256×256	64×64	29.2G	26.4M
Sekii [27]	88.1	-	-	yes	384×384	12×12	6G	16M
FPD [35]	91.1	Know. dist.	4	yes	256×256	64×64	3.6G	3.2M
HRNet [29]	92.3	-	-	yes	256×256	64×64	9.5G	28.5M
DS-Hourglass	91.5	-	8	no	256×256	64×64	4.7G	4.2M

5.3 Comparisons to State-Of-The-Art Methods

MPII Single-Person dataset From Table 3, we can find that our method is very lightweight and efficient. Our model has greatly reduced the deployment cost, while still achieving a high PCKh of 91.5%. Compared our method with the best performer, PIL [20], the DS-Hourglass needs only 16% of its computational cost but has only 0.9% drop in PCKh. Our method outperforms FPD [35] (91.5% vs 91.1% AP) which needs knowledge distillation and pretrained weights.

LSP dataset Our method also achieve the 90.8% PCK@0.2 accuracy on LSP dataset which is same as FPD [35], without using extra dataset. Because space is limited, the comparison is not listed in the form of a table.

MPII Multi-Person dataset In Table 4, we compare our method with the leading methods in recent years. It should be noted that our method does not use single-person pose estimation to refine the results. Research works [3,18] have reported that the single-pose refinement can improve the result by about 2.6%. However, the refinement is always time-consuming, so we did not use it. We get very competitive result 77.4% achieve the state-of-the-art among the methods without refinement. Our model has only 4.6M parameters and needs 13.6 GFLOPs when using input size of 384×384 . To best of our knowledge, PPN [18] is the state-of-the-art on MPII Multi-Person dataset, from our ablation Table 2, we can find that our method is better than PPN, and our method can reduced the computational cost by approximately 50GFLOPs.

Table 5 lists the results on MPII 288 test set, and our method gets 81.0%, only 0.3% lower than the best one [7] which uses refinement. It can be found that our method has great advantages in the distal part of the body (*e.g.* wrist, knee, ankle, *etc*), as we use hierarchical centroid-rooted tree to avoid long-range offset prediction.

6 Conclusions

In this paper, we develop a light-weight Hourglass network by applying depthwise separable convolution and mixed depthwise convolution. The new network can

Table 4. Results on the Full MPII Multi-Person test set.

Methods	Head	Shoulder	Elbow	Wrist	Hip	Knee	Ankle	Total	Refine.
CMU-Pose [3]	91.2	87.6	77.7	66.8	75.4	68.9	61.7	75.6	yes
AE-Pose [16]	92.1	89.3	78.9	69.8	76.2	71.6	64.7	77.5	yes
RefinePose [7]	91.8	89.5	80.4	69.6	77.3	71.7	65.5	78.0	yes
PPN [18]	92.2	89.7	82.1	74.4	78.6	76.4	69.3	80.4	yes
SPM [19]	89.7	87.4	80.4	72.4	76.7	74.9	68.3	78.5	yes
DeepCut [24]	73.4	71.8	57.9	39.9	56.7	44.0	32.0	54.1	no
DeeperCut [12]	89.4	84.5	70.4	59.3	68.9	62.7	54.6	70.0	no
Levinkov <i>et al.</i> [15]	89.8	85.2	71.8	59.6	71.1	63.0	53.5	70.6	no
ArtTrack [11]	88.8	87.0	75.9	64.9	74.2	68.8	60.5	74.3	no
RMPE [6]	88.4	86.5	78.6	70.4	74.4	73.0	65.8	76.7	no
Sekii [27]	93.9	90.2	79.0	68.7	74.8	68.7	60.5	76.6	no
DS-hourglass(mix)	91.6	88.3	78.0	68.3	77.9	72.5	65.1	77.4	no

Table 5. Results on a set of 288 images from MPII Multi-Person test set.

Methods	Head	Shoulder	Elbow	Wrist	Hip	Knee	Ankle	Total	Refine.
CMU-Pose [3]	92.9	91.3	82.3	72.6	76.0	70.9	66.8	79.0	yes
AE-Pose [16]	91.5	87.2	75.9	65.4	72.2	67.0	62.1	74.5	yes
RefinePose [7]	93.8	91.6	83.9	75.2	78.0	75.6	70.7	81.3	yes
DeepCut [24]	73.1	71.7	58.0	39.9	56.1	43.5	31.9	53.5	no
Iqbal and Gall [13]	70.0	65.2	56.4	46.1	52.7	47.9	44.5	54.7	no
DeeperCut [12]	92.1	88.5	76.4	67.8	73.6	68.7	62.3	75.6	no
ArtTrack [11]	92.2	91.3	80.8	71.4	79.1	72.6	67.8	79.3	no
RMPE [6]	89.4	88.5	81.0	75.4	73.7	75.4	66.5	78.6	no
Sekii [27]	95.2	92.2	83.2	73.8	74.8	71.3	63.4	79.1	no
DS-Hourglass(mix)	93.2	91.1	81.5	74.7	81.0	75.5	70.2	81.0	no

be directly applied to single-person pose estimation. Based on this backbone network, we further proposed an efficient multi-person pose estimation method. Both our single-person and multi-person pose estimation methods can achieve competitive accuracies on public datasets with low computational costs.

7 Acknowledgement

This work was supported in part by the Sichuan Science and Technology Program, China, under grants No.2020YFS0057, and the Fundamental Research Funds for the Central Universities under Project ZYGX2019Z015.

References

1. Andriluka, M., Pishchulin, L., Gehler, P., Schiele, B.: 2d human pose estimation: New benchmark and state of the art analysis. In: Proceedings of the IEEE Conference on Computer Vision and Pattern Recognition. pp. 3686–3693 (2014)

2. Bourdev, L., Malik, J.: Poselets: Body part detectors trained using 3d human pose annotations. In: International Conference on Computer Vision. pp. 1365–1372 (2009)
3. Cao, Z., Simon, T., Wei, S.E., Sheikh, Y.: Realtime multi-person 2d pose estimation using part affinity fields. In: Proceedings of the IEEE Conference on Computer Vision and Pattern Recognition. pp. 7291–7299 (2017)
4. Chen, Y., Wang, Z., Peng, Y., Zhang, Z., Yu, G., Sun, J.: Cascaded pyramid network for multi-person pose estimation. In: Proceedings of the IEEE Conference on Computer Vision and Pattern Recognition. pp. 7103–7112 (2018)
5. Chollet, F.: Xception: Deep learning with depthwise separable convolutions. In: Proceedings of the IEEE Conference on Computer Vision and Pattern Recognition. pp. 1251–1258 (2017)
6. Fang, H.S., Xie, S., Tai, Y.W., Lu, C.: Rmpe: Regional multi-person pose estimation. In: Proceedings of the IEEE International Conference on Computer Vision. pp. 2334–2343 (2017)
7. Fieraru, M., Khoreva, A., Pishchulin, L., Schiele, B.: Learning to refine human pose estimation. In: Proceedings of the IEEE Conference on Computer Vision and Pattern Recognition Workshops. pp. 205–214 (2018)
8. He, K., Gkioxari, G., Dollár, P., Girshick, R.: Mask r-cnn. In: Proceedings of the IEEE International Conference on Computer Vision. pp. 2961–2969 (2017)
9. He, K., Zhang, X., Ren, S., Sun, J.: Deep residual learning for image recognition. In: Proceedings of the IEEE Conference on Computer Vision and Pattern Recognition. pp. 770–778 (2016)
10. Howard, A.G., Zhu, M., Chen, B., Kalenichenko, D., Wang, W., Weyand, T., Andreetto, M., Adam, H.: Mobilenets: Efficient convolutional neural networks for mobile vision applications. arXiv preprint arXiv:1704.04861 (2017)
11. Insafutdinov, E., Andriluka, M., Pishchulin, L., Tang, S., Levinkov, E., Andres, B., Schiele, B.: Arttrack: Articulated multi-person tracking in the wild. In: Proceedings of the IEEE Conference on Computer Vision and Pattern Recognition. pp. 6457–6465 (2017)
12. Insafutdinov, E., Pishchulin, L., Andres, B., Andriluka, M., Schiele, B.: Deepercut: A deeper, stronger, and faster multi-person pose estimation model. In: European Conference on Computer Vision. pp. 34–50 (2016)
13. Iqbal, U., Gall, J.: Multi-person pose estimation with local joint-to-person associations. In: European Conference on Computer Vision. pp. 627–642 (2016)
14. Johnson, S., Everingham, M.: Clustered pose and nonlinear appearance models for human pose estimation. In: British Machine Vision Conference. vol. 2, p. 5 (2010)
15. Levinkov, E., Uhrig, J., Tang, S., Omran, M., Insafutdinov, E., Kirillov, A., Rother, C., Brox, T., Schiele, B., Andres, B.: Joint graph decomposition & node labeling: Problem, algorithms, applications. In: Proceedings of the IEEE Conference on Computer Vision and Pattern Recognition. pp. 6012–6020 (2017)
16. Newell, A., Huang, Z., Deng, J.: Associative embedding: End-to-end learning for joint detection and grouping. In: Advances in Neural Information Processing Systems. pp. 2277–2287 (2017)
17. Newell, A., Yang, K., Deng, J.: Stacked hourglass networks for human pose estimation. In: European Conference on Computer Vision. pp. 483–499 (2016)
18. Nie, X., Feng, J., Xing, J., Yan, S.: Pose partition networks for multi-person pose estimation. In: Proceedings of the European Conference on Computer Vision. pp. 684–699 (2018)

19. Nie, X., Feng, J., Zhang, J., Yan, S.: Single-stage multi-person pose machines. In: Proceedings of the IEEE International Conference on Computer Vision. pp. 6951–6960 (2019)
20. Nie, X., Feng, J., Zuo, Y., Yan, S.: Human pose estimation with parsing induced learner. In: Proceedings of the IEEE Conference on Computer Vision and Pattern Recognition. pp. 2100–2108 (2018)
21. Papandreou, G., Zhu, T., Chen, L.C., Gidaris, S., Tompson, J., Murphy, K.: Personlab: Person pose estimation and instance segmentation with a bottom-up, part-based, geometric embedding model. In: Proceedings of the European Conference on Computer Vision. pp. 269–286 (2018)
22. Papandreou, G., Zhu, T., Kanazawa, N., Toshev, A., Tompson, J., Bregler, C., Murphy, K.: Towards accurate multi-person pose estimation in the wild. In: Proceedings of the IEEE Conference on Computer Vision and Pattern Recognition. pp. 4903–4911 (2017)
23. Pham, H., Guan, M.Y., Zoph, B., Le, Q.V., Dean, J.: Efficient neural architecture search via parameter sharing. arXiv preprint arXiv:1802.03268 (2018)
24. Pishchulin, L., Insafutdinov, E., Tang, S., Andres, B., Andriluka, M., Gehler, P.V., Schiele, B.: Deepcut: Joint subset partition and labeling for multi person pose estimation. In: Proceedings of the IEEE Conference on Computer Vision and Pattern Recognition. pp. 4929–4937 (2016)
25. Ren, S., He, K., Girshick, R., Sun, J.: Faster r-cnn: Towards real-time object detection with region proposal networks. In: Proceedings of the International Conference on Neural Information Processing Systems. pp. 91–99 (2015)
26. Sandler, M., Howard, A., Zhu, M., Zhmoginov, A., Chen, L.C.: Mobilenetv2: Inverted residuals and linear bottlenecks. In: Proceedings of the IEEE Conference on Computer Vision and Pattern Recognition. pp. 4510–4520 (2018)
27. Sekii, T.: Pose proposal networks. In: Proceedings of the European Conference on Computer Vision. pp. 342–357 (2018)
28. Sifre, L., Mallat, S.: Rigid-motion scattering for image classification. Ph. D. thesis (2014)
29. Sun, K., Xiao, B., Liu, D., Wang, J.: Deep high-resolution representation learning for human pose estimation. In: Proceedings of the IEEE Conference on Computer Vision and Pattern Recognition. pp. 5693–5703 (2019)
30. Szegedy, C., Vanhoucke, V., Ioffe, S., Shlens, J., Wojna, Z.: Rethinking the inception architecture for computer vision. In: Proceedings of the IEEE Conference on Computer Vision and Pattern Recognition. pp. 2818–2826 (2016)
31. Tan, M., Le, Q.V.: Mixconv: Mixed depthwise convolutional kernels. arXiv preprint arXiv:1907.09595 (2019)
32. Tian, Z., Chen, H., Shen, C.: Directpose: Direct end-to-end multi-person pose estimation. arXiv preprint arXiv:1911.07451 (2019)
33. Wei, S.E., Ramakrishna, V., Kanade, T., Sheikh, Y.: Convolutional pose machines. In: Proceedings of the IEEE conference on Computer Vision and Pattern Recognition. pp. 4724–4732 (2016)
34. Xiao, B., Wu, H., Wei, Y.: Simple baselines for human pose estimation and tracking. In: Proceedings of the European Conference on Computer Vision. pp. 466–481 (2018)
35. Zhang, F., Zhu, X., Ye, M.: Fast human pose estimation. In: Proceedings of the IEEE Conference on Computer Vision and Pattern Recognition. pp. 3517–3526 (2019)